View Journal

Analytical Methods

Accepted Manuscript

This article can be cited before page numbers have been issued, to do this please use: A. Cruz Sotolongo, E. M. Martinis and R. G. Wuilloud, *Anal. Methods*, 2017, DOI: 10.1039/C7AY02201H.

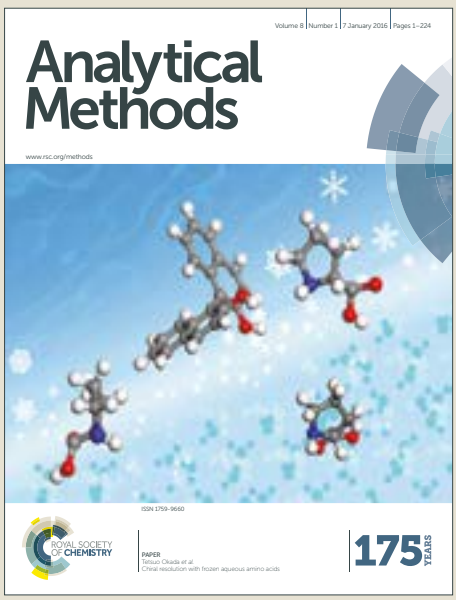

ROYAL SOCIETY OF CHEMISTRY

rsc.li/methods

View Article Online
DOI: 10.1039/C7AY02201H

An easily prepared graphene oxide-ionic liquid hybrid nanomaterial for micro-solid phase extraction and preconcentration of Hg in water samples

Annaly Cruz Sotolongo, Estefanía M. Martinis and Rodolfo G. Wuilloud*

Laboratory of Analytical Chemistry for Research and Development (QUIANID), Facultad de Ciencias Exactas y Naturales, Universidad Nacional de Cuyo, Instituto Interdisciplinario de Ciencias Básicas (ICB), UNCUYO-CONICET, Padre J. Contreras 1300, (5500) Mendoza, Argentina

*Corresponding author. Tel: +54-261-4259738

E-mail address: rwuilloud@mendoza-conicet.gob.ar; rodolfowuilloud@gmail.com

(R.G. Wuilloud)

View Article Online
DOI: 10.1039/C7AY02201H

Abstract

A preconcentration method based on the use of graphene oxide (GO) functionalized with an ionic liquid (IL) was developed for trace Hg determination in water samples. The IL-GO hybrid nanomaterial was prepared by a simple procedure to functionalize GO with the IL 1-butyl-3-dodecylimidazolium bromide ([C_4C_{12}im]Br) and its performance as a sorption material for Hg was evaluated. A microcolumn filled with the IL-GO nanomaterial was used for preconcentration and determination of Hg followed by electrothermal atomic absorption spectrometry (ETAAS) detection. Mercury was retained at pH 5.0 and 20% (v/v) HNO_3 was used for the elution of Hg from the microcolumn. The effects of different variables, including sample volume, extraction time, sample flow rate, type and concentration of eluent and eluent flow rate were carefully studied. High retention efficiency (100%) was achieved with the proposed IL-GO sorption nanomaterial without the need of additional chelating reagents or derivatization reagents, which is an important advantage compared with traditional preconcentration methods. A sensitivity enhancement factor of 100 and a low detection limit of 14 ng L^{-1} were obtained under optimal experimental conditions. The proposed method can be considered as a simple, cost-effective and efficient alternative for Hg determination in water samples like river, rain, mineral and tap water.

Keywords*: graphene oxide; 1-butyl-3-dodecylimidazolium bromide; mercury; solid phase microextraction; electrothermal atomic absorption spectrometry*

View Article Online
DOI: 10.1039/C7AY02201H

1 Introduction

Mercury is one of the most well-known toxic elements and the World Health Organization (WHO) places it among the first ten chemicals that are of major public health concern. Although regulations and efforts are exercised at various levels, Hg pollution from both natural and anthropogenic sources have remained a major safety problem.[1] Thus, water contamination of Hg could be a problem worldwide and its control must be assured by appropriate analytical methods.[2]

Several detection techniques have been used for the determination of Hg including, electrothermal atomic absorption spectrometry (ETAAS),[3] atomic fluorescence spectrometry (AFS)[4] or inductively coupled plasma mass spectrometry (ICP-MS).[5] ETAAS shows several advantages including, relative simplicity, reduced cost, and low sample volume requirements. However, since Hg concentrations are extremely low (ng L^{-1} levels) in natural waters, a preconcentration procedure must be applied. Therefore, to exploit the potential of ETAAS technique, this has to be combined with preconcentration systems involving efficient sorption materials.[6, 7] In this way, the coupling of a microcolumn filled with a high performance sorption material to ETAA yields very low detection limits and allow trace Hg determination.

Graphene is a nanomaterial formed by layers having a thickness of a few atoms and have attracted great attention due to its applications in various fields: sensors, electronics, sorption material for remediation and analytical chemistry.[8] Due to their unique physicochemical properties, this nanomaterial hold a great promise for its applications in chemical analysis.[9] Graphene has a large specific surface area (2630 m^2 g^{-1}),[10] suggesting a high sorption capacity. Furthermore, it can be easily modified to add different functional groups to its surface, e.g. by oxidation to obtain graphene oxide (GO) containing different groups (C-O, COO^-).[9] The Hummer method have been

View Article Online
DOI: 10.1039/C7AY02201H

generally employed to prepare GO due to its low cost and large scale production for analytical use.[11] However, the strength of interaction due to Van der Waals forces may inevitably result in an agglomeration of GO sheets, which compromises the overall yield of this carbon material.[12] Therefore, several types of functionalizations have been used to obtain GO with greater dispersibility.[8, 13] The functionalization approaches have been classified as covalent functionalization, noncovalent functionalization, substitutional doping, and hybridization with nanoparticles, nanowires, and other materials, considering the method and materials used.[8] Recently, Ionic Liquids (ILs) have been proposed to improve the analytical properties of GO, mainly due to the modification of its surface properties and the increase of active sites.[14] ILs are a class of organic melt salts at room temperature which completely comprise cations and anions. Due to their high conductivity, the wide potential window, the innate liquid state, low melting points and negligible vapor pressures, ILs has been applied for GO functionalization.[15] Thus, the novel IL-GO nanomaterials are expected to possess the advantages of the individual components, resulting in new, advanced adsorbents with tunable extraction capabilities and improved performance.[16] Moreover, implementation of these hybrid nanomaterials in novel microextraction techniques can result into efficient analytical methods for the determination of toxic trace elements such as Hg. In this sense, micro-solid phase extraction (μ-SPE) is a widely used technique for environmental sample pretreatment due to its high recovery, high enrichment factor, low consumption of solvents and ease of automation.[17] The sorption material determines the selectivity and sensitivity of the method and GO have demonstrated to be an effective sorbent for metal preconcentration.[18, 19] Furthermore, on-line μ-SPE preconcentration systems are advantageous for metal determination because of their flexibility, simplicity, high sample throughput and versatility.[20] In this work, a novel

View Article Online
DOI: 10.1039/C7AY02201H

preconcentration method based on the μ-SPE technique, using an IL-GO hybrid nanomaterial as sorbent and ETAAS were combined for trace Hg determination. A microcolumn filled with the new sorption material was used for preconcentration of the analyte. The main factors influencing μ-SPE and the determination of Hg such as sixe and shape of the microcolumn, sorption material load, sample pH, sample flow rate and volume, type and concentration of eluent were examined in detail. The optimum conditions were established and the determination of Hg in different types of water was successfully performed reaching a high preconcentration factor and a low LOD.

2 Material and methods

2.1 Instrumentation

Measurements were performed with a PerkinElmer (Überlingen, Germany) Model 5100 ZL atomic absorption spectrometer equipped with a transversely heated graphite atomizer and a Zeeman-effect background correction system. A Hg hollow cathode lamp (PerkinElmer) operated at a current of 170 mA and a wavelength of 228.8 nm with a spectral band width of 0.7 nm was used. All measurements were made based on absorbance signals with an integration time of 5 s. The temperature vs. time program for the atomizer is fully depicted in Table 1. A Horiba F-51 pH meter (Kyoto, Japan) was used for pH determinations. A schematic of the microextraction system is shown in Fig. 1, which consisted of: two Gilson (Villiers Le-Bell, France) Minipuls 3 peristaltic pumps, two six-port two-position injection valves (Oak Harbor, WA, USA) and a home-made microcolumn (8 mm length and 2 mm i.d.) filled with the retention material (an homogenized mixture of 6 mg of IL-GO and 54 mg of milled glass). At the two ends of the microcolumn, cotton plugs were used to avoid the loss or mixing of the sorption material. Tygon-type pump tubes (Gilson) were employed for the delivery of all

View Article Online
DOI: 10.1039/C7AY02201H

aqueous streams. Solvent-resistant pump tubes (Gilson) were used for HNO_3 solutions. The characterization of the hybrid material was performed by a Nicolete Protégé 460 Fourier transform infrared spectrometry (FT-IR) (Madison, WI, USA) and a Carl Zeiss EM900 transmission electron microscope (TEM) (Jena, Germany).

2.2 Reagents

A commercially available 1000 mg L^{-1} Hg^{2+} standard solution (Merck, Darmstadt, Germany) was used. Lower concentrations were prepared by diluting the standard solution with 0.1 mol L^{-1} HNO_3. Stock methylmercury (MeHg), ethylmercury (EtHg) and phenylmercury (PhHg) solutions (1000 mg L^{-1}) were prepared from methylmercury chloride, ethylmercury chloride and phenylmercury chloride (Merck), respectively, in methanol (Merck). Working standard solutions were prepared daily. The organomercurial solutions were stored away from light at 4 °C to prevent decomposition. Acetic acid–acetate buffer solution was prepared from a 2 mol L^{-1} acetic acid (Sigma-Aldrich, Milwaukee, WI, USA) solution adjusted to pH 5 with sodium hydroxide (Merck). Ultrapure water (18 MΩ cm) was obtained from an Osmoion-U-0.5 ultrapure water equipment (APEMA, Buenos Aires, Argentina). For the synthesis of IL, GO and IL-GO the following reagents were used: 1-butylimidazole (99%) (Fluka Buchs, Switzerland), 1-bromododecane (97%) (Sigma-Aldrich)), ethyl acetate (99.8%) (Sigma-Aldrich), graphite powder (99.99%) (Sigma-Aldrich), H_2SO_4 (95-97%) (Merck), $KMnO_4$ (99%) (Sigma-Aldrich), H_2O_2 (30%) (Sigma-Aldrich), HCl (37%) (Merck), NaOH (98%) (Sigma-Aldrich), KOH (98%) (Sigma-Aldrich) and CH_2Cl_2 (99%) (Sigma-Aldrich), thiourea (99%) (Sigma-Aldrich) and EDTA (99%) (Sigma-Aldrich) solutions were tested as eluents.

View Article Online
DOI: 10.1039/C7AY02201H

2.3 Synthesis of 1-butyl-3-dodecylimidazolium bromide

The synthesis of the IL $[C_4C_{12}im]Br$ was performed as reported by Baltazar et al. with a few modifications.[21] Briefly, a 0.10 mol 1-butylimidazole (6.5 mL) solution was mixed with 0.11 mol 1-bromododecane (13.2 mL) solution to obtain a homogeneous mixture. The mixture was heated and refluxed (70 °C) under nitrogen for 48 h, with constant stirring. The product was dissolved in 25 mL of ultrapure water and washed with six aliquots of ethyl acetate (25 mL) to purify the product. Finally, water was evaporated under vacuum at 80 ^{o}C and the IL was characterized by FT-IR technique.

2.4 Synthesis of graphene oxide

The GO was synthesized following a modified version of the Hummer's method.[11, 22] Briefly, commercial graphite powder (1.0 g) was placed into cold (10 ^{o}C) concentrated H_2SO_4 (50 mL) and $KMnO_4$ (4.0 g) was added gradually under stirring. The reaction was continued for 2 h at 10 ^{o}C. Afterwards, the mixture was stirred at 35 ^{o}C for 1 h. The solution was allowed to cool for 15 min and 100 mL of ultrapure water were added gently in an ice bath. A color change from black to intense orange was observed. Then, the mixture was stirred for 1 h water. After that, the mixture was diluted to 300 mL with ultrapure water and 10 mL of 30% (v/v) H_2O_2 were added to reduce the excess of $KMnO_4$ and it was allowed to stand for 19 h. The phase separation was observed and the orange solid was settled on the bottom. The supernatant was manually removed with a transfer pipette. In order to wash the product, 400 mL of 5% (v/v) HCl were added to remove metal ions. The solid was finally washed with ultrapure water until a pH of 5 was obtained. The supernatant was removed and GO was dried in a stove at 60 $^{\circ}$C for 5 h. The GO was characterized by FT-IR and TEM techniques.

View Article Online
DOI: 10.1039/C7AY02201H

2.5 Functionalization of graphene oxide with the ionic liquid

The functionalization of GO with the IL was performed following a procedure described by Huang et al. with slight modifications. [23] An amount of 100 mg of GO was diluted in 30 mL of ultrapure water. Then, 0.4 mL of 8 mol L^{-1} KOH were added to adjust the pH to 9. The solution was stirred for 5 h at room temperature. Subsequently, the solution was mixed with 800 mg of $[C_4C_{12}im]Br$ in 60 mL of chloroform followed by stirring for 48 h. The organic phase was separated by centrifugation and washed with CH_2Cl_2 and the functionalized nanomaterial was allowed to dry at room temperature. Finally, the IL-GO was characterized by FT-IR and TEM techniques.

2.6 Sample collection and conditioning

Different water samples including tap water, river water, bottled mineral water and rainwater collected in Mendoza province (Argentina) were analyzed in this work. For the collection of tap water samples, domestic water was allowed to run for 20 min and approximately a volume of 1000 mL was collected in a beaker. Mineral water was purchased from local supermarkets. River water samples were collected in cleaned bottles rinsed three times with water sample prior to sample collection. A sample volume of 2000 mL was collected at a depth of 5 cm of the surface. Rainwater samples were collected during a rain episode occurred in Mendoza city (Argentina) in acid-cleaned bottles that were rinsed three times with the sample prior to collection. The water samples were irradiated for 3 h with a 150 W UV lamp in order to photo-oxidize organo-Hg compounds that could be present in water.[24] All the material used in this work was previously washed with a 5% (v/v) HNO_3 solution followed by ultrapure water before drying in a clean air hood.

View Article Online
DOI: 10.1039/C7AY02201H

2.7 General μ-SPE procedure for Hg preconcentration and determination

A schematic diagram of the preconcentration system is shown in Fig. 1. The objectives of each step are summarized in Table 2. Before sample loading, the column was conditioned with 20% (v/v) HNO_3 and then with an acetic acid–acetate buffer solution to maintain the system at pH 5, driven by the peristaltic pump P_1 a flow rate of 2.5 mL min^{-1} (3 minutes). After this procedure, 5 mL of sample (S) was propelled (Step I) by pump P_1 at a flow rate of 0.3 mL min^{-1}. Simultaneously, pump P_2 supplied 20% (v/v) HNO_3 to the loop (L) of valve V_2, until it was filled. Valve V_1 and V_2 were switched to the loading position during these operations (Table 2). The pump P_2 was then switched off.

In Step II, valves V_1 and V_2 were set at the injection position and Hg retained in the microcolumn was eluted with 50 μL of 20% (v/v) HNO_3. The eluent was supplied at a flow rate of 0.3 mL min^{-1}. Subsequently, the eluate was diluted to 100 μL with ultrapure water. The concentration of Hg was determined by ETAAS, injecting 40 μL of the diluted eluate into the graphite furnace. Instrumental conditions for ETAAS determination are mentioned in Table 1.

Calibration was performed with aqueous standards subjected to the same preconcentration procedure. Blank solutions were analyzed in the same way as standard and sample solutions.

3 Results and discussion

3.1 Morphology and structural characteristics of IL, GO and IL-GO

FT-IR technique was employed for the characterization of IL, GO and IL-GO. Spectra were measured in the range from 4000 to 400 cm^{-1} with a resolution of 4 cm^{-1}. FT-IR spectra of IL-GO (red), GO (blue) and IL (light blue) are shown in Fig. 2. To

View Article Online
DOI: 10.1039/C7AY02201H

obtain the FT-IR spectra of GO, the KBr pellet method was used with a mass proportion of 3% of the sample homogeneously dispersed in KBr. The GO spectrum was similar to others reported in the literature.[25] This showed a significant shift of the stretching vibration of the hydroxyl groups (O-H, C=O, C=C, C-OH, C-O), attributed to the presence of these groups on the surface, with lower degree of association. A drop of $[C_4C_{12}im]Br$ was deposited on the KBr pellet to obtain the IL spectra. It exhibited a typical strong peak centered at approximately 1494 cm^{-1} corresponding to the draw frequency of the functional group -C=N, while both peaks at 1168 and 1540 cm^{-1} were attributed to the stretching vibration of the imidazole ring.

The spectrum of IL-GO hybrid nanomaterial was also obtained by the KBr pellet technique. From the comparison of IL and IL-GO spectra, a very coincident band pattern was observed. The asymmetric ring stretching in the resulting plane of the imidazolium ring resulted in a peak at 1164 cm^{-1}, which indicated that functionalization of GO with the IL was successful. On the other hand, the characteristic band of GO for C=O (1735-1720 cm^{-1}) bond was not observed in the spectrum of IL-GO so the formation of a carboxylate (1595 cm^{-1}) was suggested. The characteristic bands observed were: aromatic C=C (1615 cm^{-1}), epoxy C-OH (1225 cm^{-1}) and alkoxy C-O (1050 cm^{-1}). The oxygen-containing functional groups and the imidazole were confirmed in the FT-IR spectrum of the IL-GO hybrid nanomaterial. Moreover, functionalization of GO with this type of IL could proceed thanks to ionic interactions, electrostatic and Van der Waals forces, which are the most common interactions occurring on the surface of GO with charged functional groups. Moreover, IL molecules could be adsorbed on GO by interaction with carboxyl groups occurring on the surface of this nanomaterial.[23]

For TEM characterization, GO and IL-GO were dispersed by sonication into

View Article Online
DOI: 10.1039/C7AY02201H

water at a concentration of 0.1 mg mL^{-1}. A drop of the dispersions were placed directly on two copper grids, dried at room temperature and TEM images were obtained working with the microscope at 80 kV, with a high-resolution Gatan SC1000-832 CCD camera. The Fig. 3a shows that GO formed sheets that were mostly dispersed in a single layer and were smooth and transparent. The TEM image of IL-GO (Fig. 3b) shows that functionalization of GO provided a layer of IL on the surface material. Although this process partially flattened the wrinkles on the GO sheets, the bound IL produced a corrugated surface. Therefore, it was proposed that the IL-GO hybrid nanomaterial could have excellent sorption performance due to the increase of the effective surface area and active sites.

3.2 Characteristics of the microcolumn and the filling material

The preparation and dimensions of the microcolumn are key factors due to the tendency of graphene-related materials to aggregate, which negatively affects the hydrodynamic characteristics of the packed column, sample flow rate and ultimately, analysis frequency.[26] For this reason, the preparation of the microcolumn was studied in detail. A careful evaluation of the optimum dimensions of the microcolumn and special characteristics of the filling material were performed. Thus, different materials with an average particle size of 710 nm like feldspar, quartz and milled glass were tested to avoid the compaction of IL-GO nanomaterial and allow solutions to flow through the microcolumn. According to the results, milled glass was the best material because it avoided the aggregation of the sorbent inside the microcolumn, preventing high back-pressures in the system. Additionally, it has excellent chemical compatibility with the mineral acids used in this work for the elution of Hg. An optimal weight proportion consisting of ~90% of milled glass and ~10% of IL-GO hybrid nanomaterial was

View Article Online
DOI: 10.1039/C7AY02201H

applied. This proportion was suitable to prevent the compaction of IL-GO nanomaterial inside the column.

Furthermore, the effects of microcolumn dimensions on the retention and elution of the analyte were studied. The length of the microcolumn was assayed in the range of 5 - 15 mm, while the internal diameter (i.d.) in the range of 2 - 5 mm. The highest Hg retention and efficient elution were achieved when the sorption material was packed in a microcolumn of 2 mm i.d. and 8 mm length.

3.3 Evaluation of ETAAS conditions for Hg determination

A careful study of the conditions for ETAAS determination was necessary due to the high volatility of Hg. Chemical modifiers were necessary to avoid deterioration of Hg sensitivity by losses of the target metal during drying and pyrolysis steps. Different amounts of $Mg(NO_3)_2$ and $Pd(NO_3)_2$ and their mixtures were assayed as chemical modifiers. The stabilization of Hg in the atomizer by Pd (20 μg) was the most effective approach as noble metals form stable amalgams with Hg.[27]

The effect of pyrolysis temperature was studied in the range of 150 - 330 °C (Fig. 1S in Supplementary Information). In this case, Hg was measured up to 250 °C without significant losses and reduced background absorption during atomization. Therefore, 250 °C was chosen as the pyrolysis temperature. Likewise, the effect of atomization temperature on Hg absorption signal was studied within the range of 800 - 1500 °C (Fig. 2S in Supplementary Information). The highest absorbance signal was achieved at 1300 °C. The ramp and hold times for pyrolysis step were studied, 10 and 20 seconds was chosen respectively. Final conditions for ETAAS detection are shown in Table 1.

View Article Online
DOI: 10.1039/C7AY02201H

3.4 Optimization of the preconcentration procedure

Several parameters affecting Hg preconcentration including pH, sample volume, extraction time, sample flow rate, eluent type and concentration and eluent flow rate were carefully studied and optimized. The study of the preconcentration variables was performed by the univariate method. All parameters mentioned above were assayed with Hg aqueous standards prepared at known concentrations of the element.

3.4.1 Influence of pH on Hg retention

In order to evaluate the effect of pH on the process, a series of standard solutions at 0.5 μg L^{-1} Hg concentration were adjusted at different pH values (1.0 - 11.0) and the proposed preconcentration method was applied. The pH was adjusted by dropwise addition of 1 mol L^{-1} HCl or NaOH solutions. The main mechanism of Hg retention on the IL-GO hybrid material might proceed by electrostatic interactions between metal ions and oxygen functional groups (–COO– and –O–). Therefore, Hg retention could be mainly determined by the nature and the concentration of these groups on the surface of the IL-GO hybrid nanomaterial.[28] Likewise, a cation exchange mechanism between Hg^{+2} and the imidazolium cation of the IL could be considered. Previous works have proposed that the transfer rate of Hg^{+2} into the IL phase increases with the length of the alkyl chain of the imidazolium ring, meaning that when longer alkyl chains are present in the imidazolium ring, the extraction of Hg could be more efficient. Thus, the extraction of Hg was increased 20% compared to the extraction obtained with GO under the same experimental conditions.[29]

The retention of Hg on the IL-GO nanomaterial was evaluated at different pHs (Fig. 3S in Supplementary Information). A constant 100% retention efficiency was obtained for Hg when the pH was increased up to 7 and after this value the retention

View Article Online
DOI: 10.1039/C7AY02201H

started to diminish (60% for pH 11). The decrease in the retention of Hg can be attributed to the hydrolysis of the metal. According to these experiments, pH 5 was selected for further experiments because of the convenience of sample preparation using the acetic acid–acetate buffer solution. In order to avoid the use of additional reagents, the pH was adjusted using an acetic-acetate buffer solution.

3.4.2 Type of eluent and concentration

The desorption of Hg from the microcolumn was studied using different acids solutions since decreasing the pH could lead to removal of Hg from the hybrid nanomaterial into the aqueous phase. Moreover, a possible mechanism to explain the elution of Hg from the sorption material could be attributed to a cation exchange mechanism between Hg^{2+} and H^{+}.[26] In order to determine the type and volume of eluent required for Hg removal from the microcolumn, 500 µL of different inorganic acids (HCl and HNO_3), EDTA and a mixture of thiourea and HCl were evaluated (Fig. 4). As a result, a 100% elution of Hg from the microcolumn was observed with 20% (v/v) HNO_3. Thus, HNO_3 was selected as eluent to promote the desorption of Hg from the IL-GO nanomaterial. Furthermore, the effect of the volume of eluent on Hg removal was investigated (25-1000 µL). It could be determined that Hg was quantitatively eluted from the microcolumn with only 50 µL of 20% (v/v) HNO_3. In addition, the best results were obtained when the elution of the analyte was developed in countercurrent mode through the microcolumn, which contributed to obtain a more efficient elution by minimizing the dispersion of the analyte.[30]

3.4.3 Influence of sample volume and flow rate

The sample volume is an important variable since it affects frequency of analysis, enhancement factor and consumption index of preconcentration methods.

View Article Online
DOI: 10.1039/C7AY02201H

Therefore, the effect of sample volume on analyte retention was evaluated in a range of 1 – 10 mL. The results showed that a sample volume of 5 mL was optimum for analysis. When higher volumes were applied, the retention of the analyte in the microcolumn decreased significantly. Therefore, a volume of 5 mL of sample was selected (Fig. 5a).

Also, sample flow rate through the microcolumn was crucial to be optimized in the preconcentration system as sensitivity of the method and enhancement factor were directly related to this variable. Sample flow rate influences the contact time between the analyte and the sorption material, consequently the dynamic sorption capacity of the microcolumn could be affected too. The effect of sample loading flow rate on Hg retention was studied in the range of 0.3 – 7 mL min^{-1}, while the elution flow rate was kept constant at 7 mL min^{-1} and the sample volume was 5 mL. The experimental results showed that the analytical signal decreased upon an increase of the sample flow rate, with a maximum at 0.3 mL min^{-1} (Fig. 5b). The almost linear decrease in absorbance signal within the tested range revealed the analyte followed a slow, but effective, mass transfer process from the IL-GO nanomaterial into the eluent, which led to quantitative removal from the microcolumn.

The influence of the elution flow rate on the removal of Hg was also examined within the range of 0.3 – 7 ml min^{-1}. Mercury was less recovered upon increasing the elution flow rate (Fig. 5c). Therefore, a flow rate of 0.3 ml min^{-1} was chosen for sample loading and elution of Hg from the microcolumn.

3.5 Microcolumn re-utilization and sorption capacity

Stability and regeneration of the IL-GO sorption material were also investigated. It was observed that the micro-column could be re-used after regeneration with 5 mL of 20% (v/v) HNO_3, followed by a washing with ultrapure water. The microcolumn was

View Article Online
DOI: 10.1039/C7AY02201H

stable without deterioration of Hg retention and capacity. This study comprised at least 100 preconcentration-elution cycles.

In addition, it was evaluated the dynamic sorption capacity of the microcolumn, which is defined as the maximum amount of analyte retained when the active sites of the IL-GO nanomaterial were saturated. In that experiment, a 0.1 mg L^{-1} Hg solution was loaded into the microcolumn at 0.3 mL min^{-1}. Simultaneously, aliquots of 500 µL of effluent were collected every 2 min in centrifuge tubes and Hg was determined in each aliquot. Mercury was efficiently retained in the microcolumn up to 20 mL of the 0.1 mg L^{-1} Hg solution was loaded. Therefore, the calculated dynamic sorption capacity of the IL-GO nanomaterial was 0.033 mg of Hg per g of IL-GO nanomaterial.

3.6 Interference study

The ionic strength effect on Hg retention was evaluated within a range of 0 – 1 mol L^{-1} $NaNO_3$. It was observed that the ionic strength did not influence the performance of the preconcentration system within the studied range. Likewise, the effect of concomitant ions regularly found in natural water samples was evaluated. This experiment was performed by analyzing 3 mL of 0.5 mg L^{-1} Hg solution containing concomitant ions at different concentrations. A concomitant ion was considered to interfere if it resulted in an analytical signal variation of ±5%. It was determined that Cu^{2+}, Zn^{2+}, Ni^{2+}, Co^{2+}, Mn^{+2} and Fe^{3+} could be tolerated up to at least 100 mg L^{-1}. Analytical signal of the blank was not modified in the presence of the concomitant ions assayed.

Furthermore, the retention of organic Hg species on the IL-GO hybrid nanomaterial was evaluated and different yields were obtained: MeHg (57%), PhHg (89%) and EtHg (83%). Therefore, since the IL-GO nanomaterial was not selective to

View Article Online
DOI: 10.1039/C7AY02201H

Hg species, and their retention was different depending on each species, a photooxidation process was applied to ensure that all organic species were transformed into inorganic Hg species before preconcentration.

3.7 Analytical performance and determination of Hg in real samples

Several parameters characterizing the performance of the preconcentration method were studied. A 100% retention efficiency was achieved for Hg under the optimal experimental conditions (Table 1). The relative standard deviation (RSD) resulting from the analysis of 10 replicates of 5 mL of a solution at 0.5 μg Hg L^{-1} was 3.9%. Also, the sensitivity enhancement factor (EF) was obtained from the ratio of the calibration curve slopes for Hg with and without application of the preconcentration method. Calibration curve without preconcentration was obtained by direct injection of 20 μL of Hg standard solutions into ETAAS at different concentrations. The regression equation obtained for the calibration curve obtained without preconcentration was $A = 0.00185C + 0.09$, where A is the absorbance and C is the concentration of Hg in μg L^{-1}. Also, the calibration curve obtained after preconcentration was linear with a correlation coefficient of 0.9987 from levels near the detection limits and up to at least 8 μg L^{-1}. The regression equation was $A = 0.185C + 0.0011$. Thus, an EF = 100 was achieved in this work when the two values of analytical sensitivity are compared. The limit of detection (LOD) obtained after preconcentration was calculated based on the signal at the intercept and three times the standard deviation about regression of the calibration curve.[30] A LOD of 14 ng L^{-1} Hg was obtained and the analysis frequency was 3 samples h^{-1}.

The accuracy of the proposed method was evaluated by analysis of a certified reference material (CRM), NIST-SRM 1641e (total Hg in water) with a Hg

View Article Online
DOI: 10.1039/C7AY02201H

concentration of 0.1016 ± 0.0017 mg L^{-1}. The concentration of Hg found in this CRM after applying the proposed method was 0.1025 ± 0.0019 mg L^{-1} indicating an acceptable accuracy of the method ($p < 0.01$). Likewise, the method was applied for the determination of Hg in different water samples collected in Mendoza province (Argentina). Concentrations of Hg in water samples were in the range of <LOD for tap water, <LOD – 0.05 μg L^{-1} for mineral water, 0.06 – 0.08 μg L^{-1} for rain water and 0.09 – 0.13 μg L^{-1} for river water. A recovery study was also developed on samples spiked at known concentration of Hg. The results are shown in Table 3. Recoveries of Hg varied between 95.6% and 105%.

Finally, a comparison with other methods reported in the literature for Hg determination is given in Table 4. In this work, an easily prepared sorbent nanomaterial implemented in a flow μ-SPE technique allowed to obtain a simple and effective microscale sample preparation technique. The high retention capacity shown by the sorbent material allowed trace Hg determination with a minimal amount of sorbent. The proposed method required a low volume of sample, which also diminished waste generation in the analytical laboratory. In addition, the proposed method showed a low LOD and a higher enhancement factor than other works. This method can be considered as a cost-effective and selective approach for trace Hg determination.

4 Conclusions

The low concentrations of Hg occurring in water samples determine that preconcentration must be applied when ETAAS detection is intended to be used for trace element determination. A sensitive analytical methodology was developed in this work for Hg preconcentration and determination in different water samples at trace levels (ng L^{-1}) using a novel IL-GO sorption material. The prepared IL-GO hybrid

View Article Online
DOI: 10.1039/C7AY02201H

nanomaterial showed excellent retention efficiency and can be used for several preconcentration-elution cycles without deterioration of the retention efficiency. The use of an IL containing long alkyl chain groups increased the retention efficiency of GO for the analyte, thus providing additional physicochemical properties that were useful for the extraction of Hg and its determination at trace levels. The mixing of IL-GO nanomaterial with milled glass prevented agglomerations and overpressures in the microcolumn. Furthermore, the μ-SPE preconcentration system can be proposed as an environmentally friendly approach as no volatile organic solvent was required during analysis and minimal amounts of reagents were used. The preconcentration method allowed Hg determination in river, rain, mineral and tap water samples with high accuracy and reproducibility.

Acknowledgements

This work was supported by Consejo Nacional de Investigaciones Científicas y Técnicas (CONICET), Agencia Nacional de Promoción Científica y Tecnológica (FONCYT) (Project PICT2013-0072-BID) and Universidad Nacional de Cuyo (Projects 06/M099 and 06/M039) (Argentina).

View Article Online
DOI: 10.1039/C7AY02201H

References

1. A. Bhan and N.N.Sarkar, *Rev. Environ. Health*, 2005, **20**, 39–56.
2. H. İ. Ulusoy, *J. AOAC Int.*, 2014, **97**, 238–244.
3. M. A. Kamyabi and A. Aghaei, *Spectrochim. Acta Part B At. Spectrosc.*, 2017, **128**, 17–21.
4. K. Huang, K. Xu, X. Hou, Y. Jia, C. Zheng and L. Yang, *J. Anal. At. Spectrom.*, 2013, **28**, 510–515.
5. F. Moreno, T. García-Barrera and J. L. Gómez-Ariza, *J. Chromatogr. A*, 2013, **1300**, 43–50.
6. E. Vereda Alonso, M. D. M. Guerrero, P. Colorado Cueto, J. Barreno Benítez, J. M. Cano Pavón and A. García De Torres, *Talanta*, 2016, **153**, 228–239.
7. I. López-García, Y. Vicente-Martínez and M. Hernández-Córdoba, *J. Anal. At. Spectrom.*, 2015, **30**, 1980–1987.
8. V. Georgakilas, M. Otyepka, A. B. B. V. Chandra, N. Kim, K. C. Kemp, P. Hobza, R. Zboril and K. S. Kim, *Chem. Rev.*, 2012, **112**, 6156−6214.
9. Q. Liu, J. Shi, L. Zeng, T. Wang, Y. Cai and G. Jiang, *J. Chromatogr. A*, 2011, **1218**, 197–204.
10. T. Zhan, Z. Tan, X. Tian and W. Hou, *Sens. Actuators, B*, 2017, **246**, 638–646.
11. L. Shahriary and A. a. Athawale, *Int. J. Renew. Energy Environ. Eng.*, 2014, **02**, 58–63.
12. H. Yang, F. Li, C. Shan, D. Han, Q. Zhang, L. Niu and A. Ivaskab, *J. Mater. Chem.*, 2009, **19**, 4632–4638.
13. A. Chinnappan, R. Appiah-Ntiamoah, W.-J. Chung and H. Kim, *Int. J. Hydrogen Energy*, 2016, **41**, 14491–14497.
14. M. Wu, Y. Ai, B. Zeng and F. Zhao, *J. Chromatogr. A*, 2016, **1427**, 1–7.
15. R. Liu, J.-f. Liu, Y.-g. Yin, X.-l. Hu and G.-b. Jiang, *Anal. Bioanal. Chem.*, 2009, **393**, 871–883.
16. M. Serrano, T. Chatzimitakos, M. Gallego and C. D. Stalikas, *J. Chromatogr. A*, 2016, **1436**, 9–18.
17. H. Piri-Moghadam, F. Ahmadi and J. Pawliszyn, *Trends Anal. Chem.*, 2016, **85**, 133–143.
18. Y. Wang, S. Gao, X. Zang, J. Li and J. Ma, *Anal. Chim. Acta*, 2012, **716**, 112–118.
19. S. Palanisamya, K. Thangavelua, S.-M. Chena, V. Velusamyb, M.-H. Changa, T.-W. Chena, F. M. A. Al-Hemaidc, M. A. Alic and S. K. Ramaraj, *Sens. Actuators, B*, 2017, **243**, 888–894.
20. L. B. Escudero, R. A. Olsina and R. G. Wuilloud, *Talanta*, 2013, **116**, 133–140.
21. Q. Q. Baltazar, J. Chandawalla, K. Sawyer and J. L. Anderson, *Colloids Surf., A*, 2007, **302**, 150–156.
22. J. Chen, B. Yao, C. Li and G. Shi, *Carbon*, 2013, **64**, 225–229.
23. W. Yan, Y. Huang, Y. Xu, L. Huang and Y. Chen, *J. Nanosci. Nanotechnol.*, 2012, **12**, 2270–2277.
24. J. C. A. de Wuilloud, R. G. Wuilloud, M. a. F. Silva, R. A. Olsina and L. D. Martinez, *Spectrochim. Acta Part B At. Spectrosc.*, 2002, **57**, 365–374.
25. A. M. Dimiev and J. M. Tour, *ACS Nano*, 2014, **8**, 3060–3068.
26. B. Parodi, A. Londonio, G. Polla, M. Savio and P. Smichowski, *J. Anal. At. Spectrom.*, 2014, **29**, 880–885.
27. A. F. d. Silva, B. Welz and A. J. Curtius, *Spectrochim. Acta Part B At. Spectrosc.*, 2002, **57**, 2031–2045.

View Article Online
DOI: 10.1039/C7AY02201H

28. B. Parodi, A. Londonio, G. Polla, M. Savio and P. Smichowski, *J Anal. At. Spectrom*, 2014, **29**, 880–885.
29. M. V. Mancini, N. Spreti, P. D. Profio and R. Germani, *Sep. Purif. Technol.*, 2013, **116**, 294-299.
30. P. Berton, E. M. Martinis and R. G. Wuilloud, *J. Hazard. Mater.*, 2010, **176**, 721-728.
31. C. He, G. Cheng, C. Zheng, L. Wu, Y.-I. Lee and X. Hou, *Anal. Methods*, 2015, **7**, 3015.
32. C. Mitani, A. Kotzamanidou and A. N. Anthemidis, *J. Anal. At. Spectrom*, 2014, **29**, 1491.
33. D. M. Abadi, M. Chamsaz, M. H. Arbab-Zavar and S. A. Taheri, *Asian J. Chem.*, 2012, **24**, 4277-4280.

View Article Online
DOI: 10.1039/C7AY02201H

Figure captions

Fig. 1 Flow injection device and its operation sequence for μ-SPE preconcentration and determination of Hg. P_1 and P_2: peristaltic pumps; V_1 and V_2: injection valves; L: solvent loop; S: sample; E: eluent; A: air; W: waste.

Fig. 2 FT-IR spectra of IL (—), GO (....) and IL-GO (—).

Fig. 3 TEM images of **a)** GO and **b**) IL-GO.

Fig. 4 Influence of the type and concentration of eluent on Hg desorption from the column: 1) 15% (v/v) HCl; 2) 30% (v/v) HCl; 3) 0.25 mol L^{-1} EDTA; 4) 20% (v/v) HCl / 5% (w/v) Thiourea; 5) 40% (v/v) HNO_3; 6) 20% (v/v) HNO_3. All experiments were performed in triplicate. Other conditions were as mentioned in Table 1.

Fig. 5 Effect of different variables on the analytical performance of the system**:** a) Sample volume, b) Sample flow rate, c) Eluent flow rate. Other conditions were as indicated in Table 1.

View Article Online
DOI: 10.1039/C7AY02201H

Table 1

Instrumental and experimental conditions for Hg determination.

Wavelength	228.8 nm
Spectral band width	0.7 nm
Lamp (EDL) current	170 mA
Injection volume	40 µL
Matrix modifier	20 µg Pd [as $Pd(NO_3)_2$]

Graphite furnace temperature program

Step	T (ºC)	Ramp time (s)	Hold time (s)	Argon flow (mL min^{-1})
Drying 1	110	1	30	250
Drying 2	130	15	15	250
Pyrolysis 1	250	10	20	250
Atomization	1300	0	5	0
Cleaning	2400	1	2	250

Optimal µ-SPE conditions

Working pH	5.0
Sample volume	5.0 mL
Eluent solvent	20% (v/v) HNO_3
Eluent volume	50 µL
Loading flow rate	0.3 mL min^{-1}
Elution flow rate	0.3 mL min^{-1}

View Article Online
DOI: 10.1039/C7AY02201H

Table 2
Operating parameters and sequence of the μ-SPE system.[a]

Step	Flow rate (mL min^{-1})	Sample volume (mL)	Time (min)	Active pump	Valve positions V_1 V_2		Purpose
I	2.5	5	2	P_1	L	L	Column conditioning
I	0.3	5	16.7	P_1-P_2	L	L	Sample and eluent loading
II	0.3	0.1	0.3	P_2	I	I	Analyte elution

[a] Refer to Fig. 1

View Article Online
DOI: 10.1039/C7AY02201H

Table 3
Determination of Hg in water samples and analyte recovery.

Sample	Hg added ($\mu g\ L^{-1}$)	Hg found ($\mu g\ L^{-1}$)	Recovery (%)[a]
Mineral water 1	-	<LOD	
	0.5	0.51±0.02	102
	1	0.99±0.03	99.0
Mineral water 2	-	0.05±0.02	
	0.5	0.54±0.02	98.0
	1	1.07±0.04	102
Tap water 1	-	<LOD	-
	0.5	0.49±0.02	98.0
	1	1.03±0.03	103
Tap water 2	-	<LOD	-
	0.5	0.50±0.02	100
	1	0.99±0.03	99.0
Rain water 1	-	0.06±0.01	-
	0.5	0.58±0.02	104
	1	1.04±0.04	98.0
Rain water 2	-	0.08±0.01	-
	0.5	0.56±0.02	96.0
	1	1.07±0.04	99.0
River water 1	-	0.09±0.01	-
	0.5	0.57±0.02	96.0
	1	1.09±0.03	100
River water 2	-	0.13±0.01	-
	0.5	0.64±0.02	102
	1	1.09±0.03	96.0

[a]100 x [(Found-base) / added]

View Article Online
DOI: 10.1039/C7AY02201H

604

Table 4

Comparison of the developed methodology with others reported for Hg determination in water.

Method	LOD (ng L^{-1})	RSD (%)	Sensitivity enhancement factor	Sample consumption (mL)	Ref.
HF-LPME/HPLC-ICP-MS[a]	110-230	-	27-48	-	5
EME[b]-ETAAS	500	6.2-7.1	102-108	-	3
Photo-CVG[c]-ETAAS	20	5	-	7	31
LIS-SH-SDME[d]-ETAAS	480	4.2	75	-	32
CPE[e]-ETAAS	1200	4.7	-	-	33
μ-SPE-ETAAS	14	3.9	100	5	Proposed method

[a]EME: Hollow fiber-liquid phase microextraction /high performance liquid chromatography- inductively coupled plasma mass spectrometry
[b]EME: Electromembrane extraction
[c]Photo-CVG: Photochemical vapor generation
[d]LIS-SH-SDME: Automated headspace single drop microextraction
[e]CPE: cloud point extraction

View Article Online
DOI: 10.1039/C7AY02201H

Fig. 1

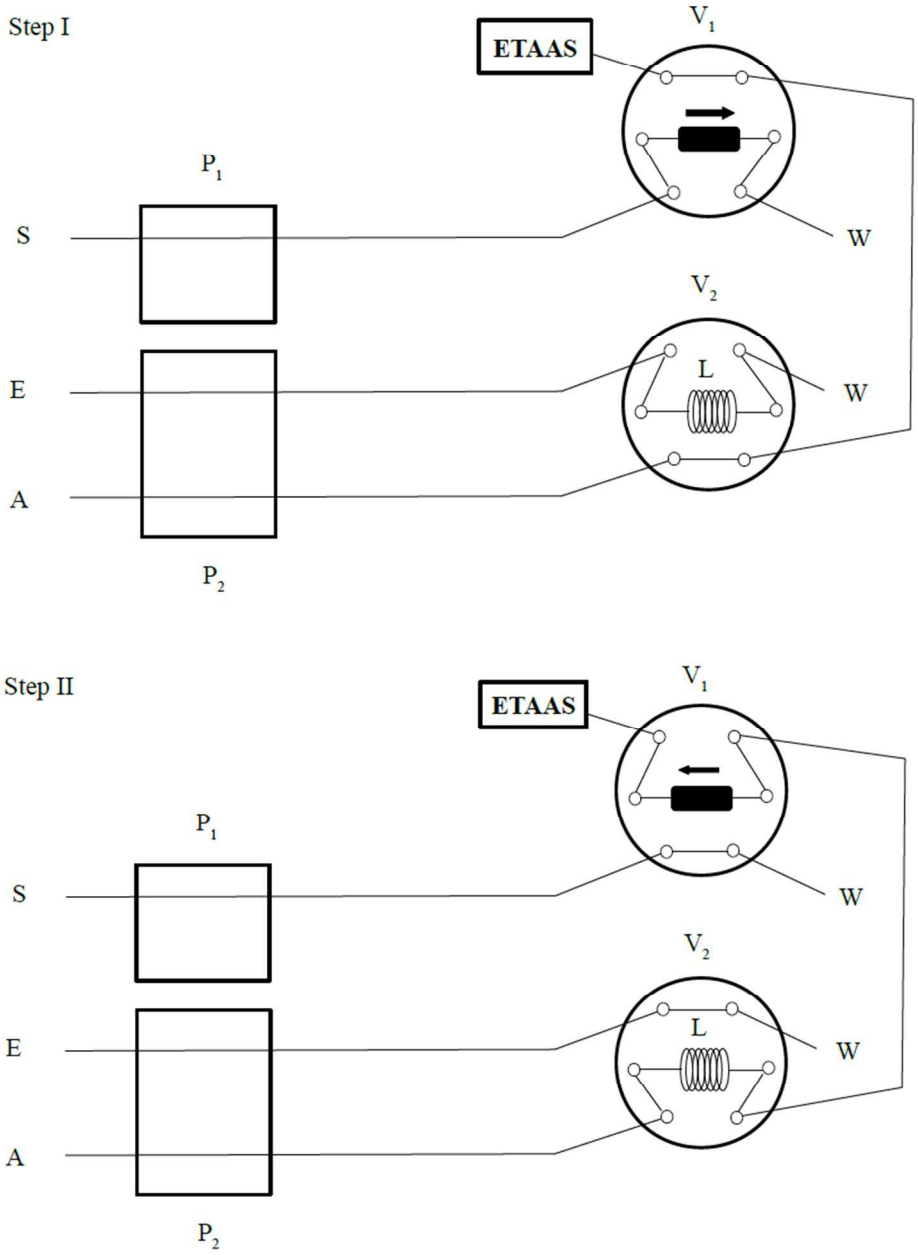

View Article Online
DOI: 10.1039/C7AY02201H

Fig. 2

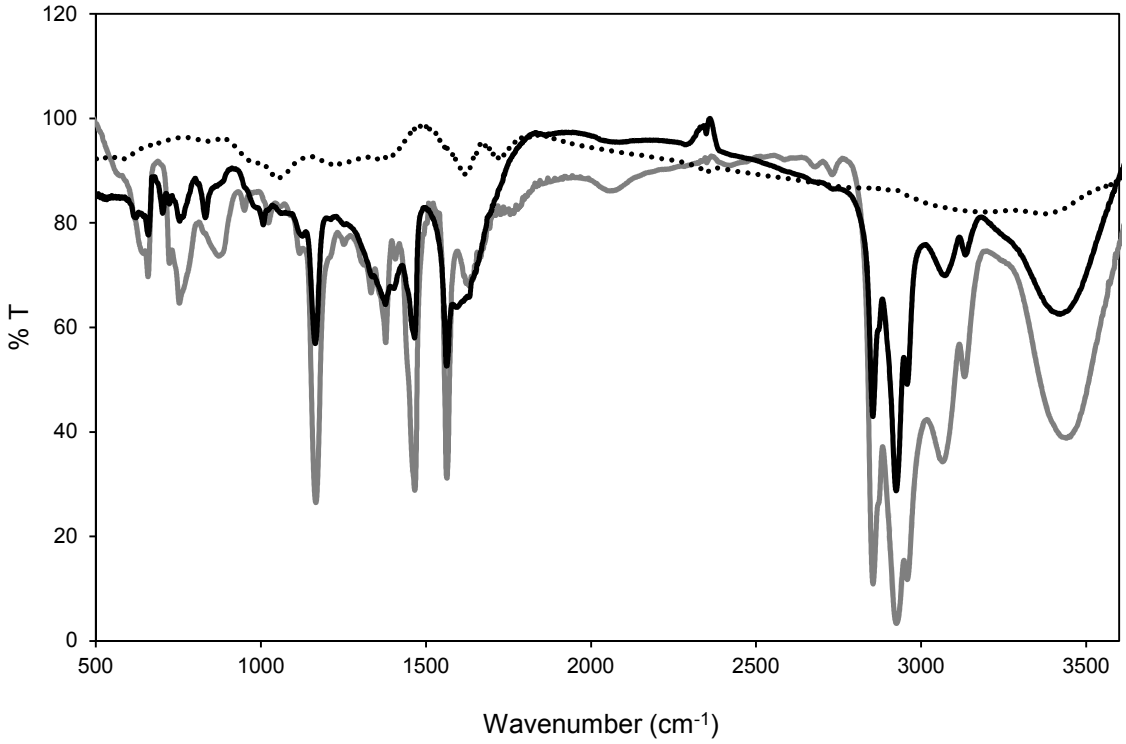

View Article Online
DOI: 10.1039/C7AY02201H

Fig. 3a

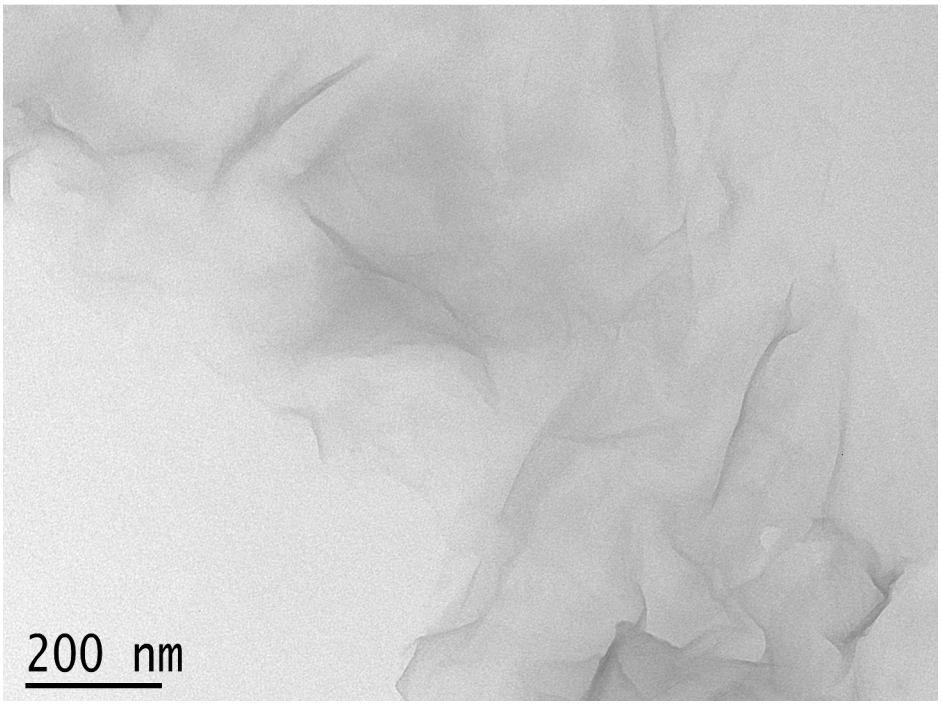

Fig. 3b

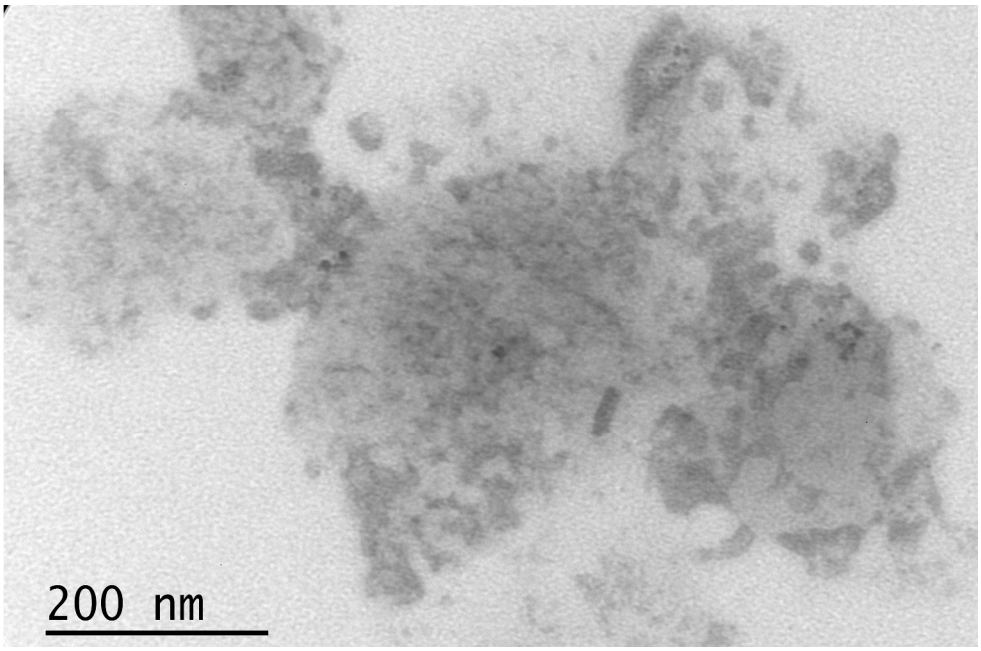

View Article Online
DOI: 10.1039/C7AY02201H

Fig. 4

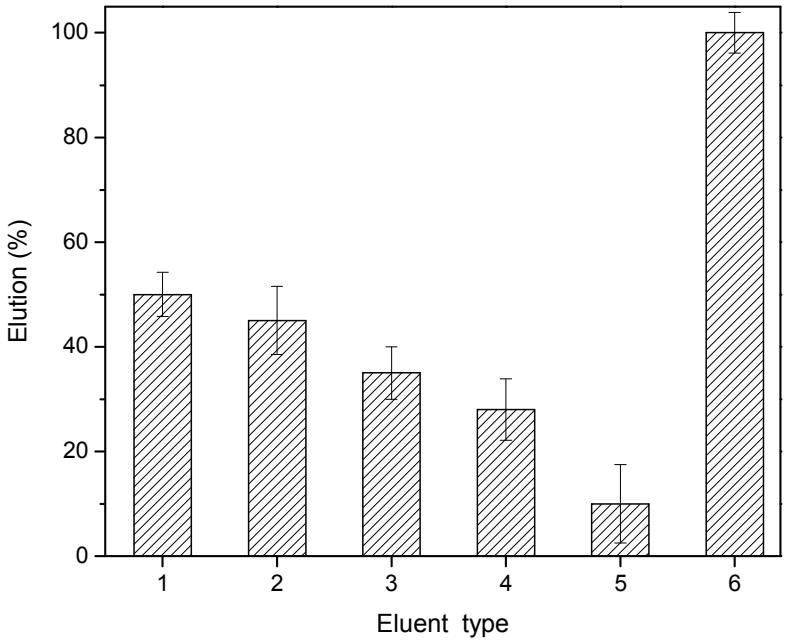

View Article Online
DOI: 10.1039/C7AY02201H

Fig. 5

(a)

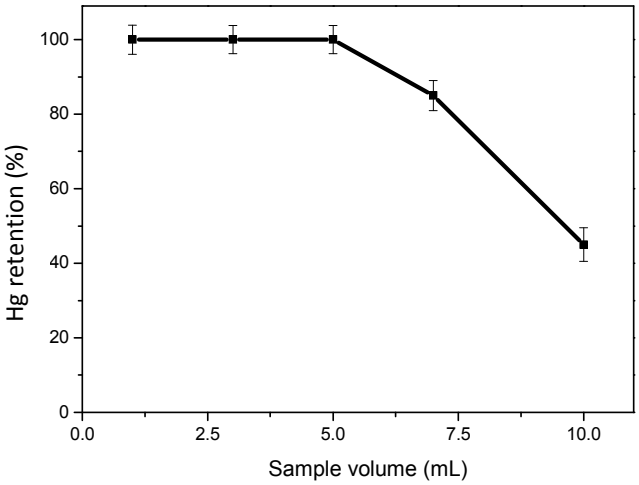

(b)

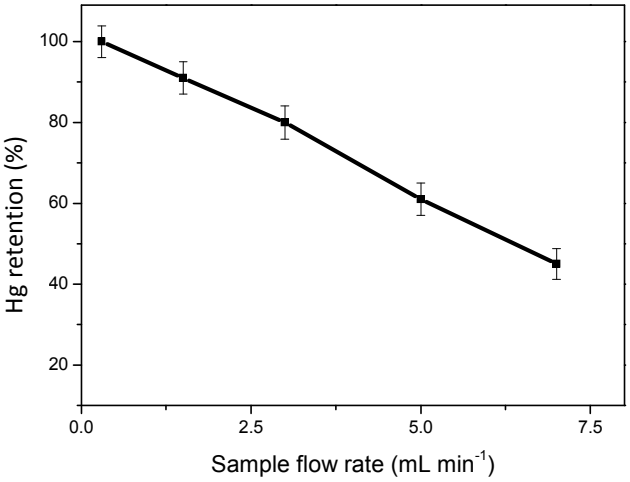

(c)

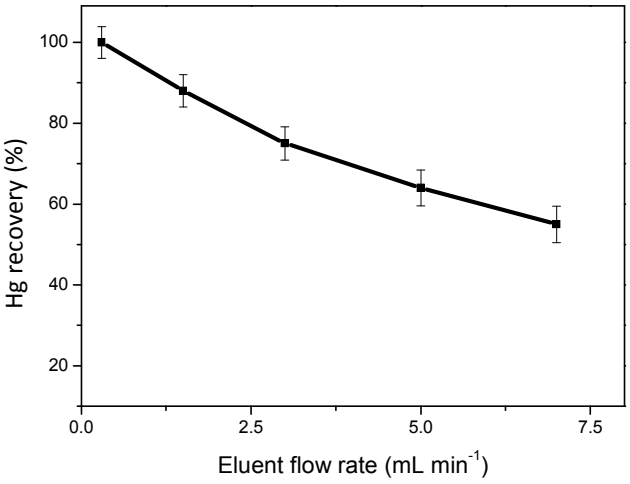

View Article Online
DOI: 10.1039/C7AY02201H

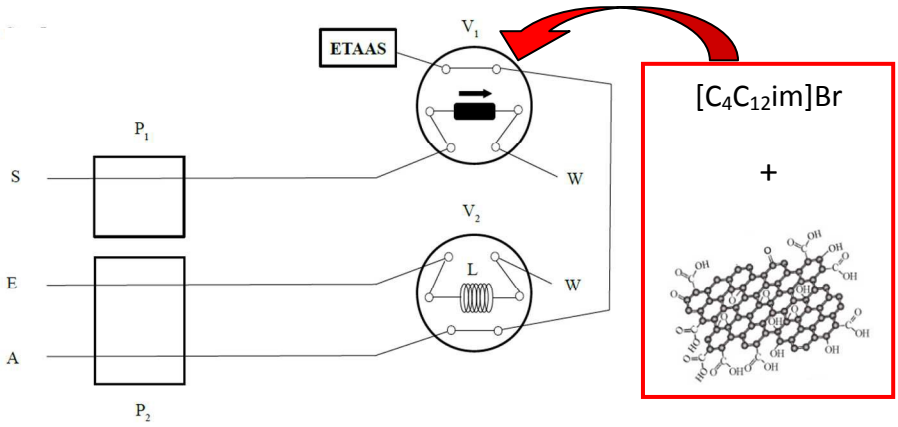

Entry:

High retention of Hg and sensitive determination with a graphene oxide-ionic liquid hybrid nanomaterial.